Astron. Astrophys. 326, 1241–1251 (1997)

ASTRONOMY
AND
ASTROPHYSICS

Absorption of magnetosonic waves in presence of resonant slow waves in the solar atmosphere

V.M. Čadež⋆, Á. Csík⋆⋆, R. Erdélyi⋆⋆⋆, and M. Goossens

Center for Plasma-Astrophysics, K.U. Leuven, Celestijnenlaan 200 B, B-3001 Heverlee, Belgium

Received 10 March 1997 / Accepted 12 May 1997

Abstract. The resonant absorption of slow and fast magnetosonic waves in a nonuniform magnetic plasma is studied for a simple planar equilibrium model. Propagating slow and fast magnetosonic waves are launched upwards in a lower uniform layer. They are partially absorbed by coupling to local resonant waves in an overlying nonuniform plasma layer at the magnetic surface where the frequency of the incoming wave equals the local Alfvén continuum frequency or the local slow continuum frequency.

The slow magnetosonic waves can only be coupled to resonant slow continuum waves. For the fast magnetosonic waves there are three possibilities as they can be coupled to resonant Alfvén continuum waves alone, resonant Alfvén continuum waves combined with resonant slow continuum waves, and resonant slow continuum waves alone. The present paper focuses on the absorption of magnetosonic waves by coupling to resonant slow continuum waves either alone or in combination with resonant Alfvén continuum waves.

The results show that the resonant absorption of slow and fast magnetosonic waves at the slow resonance position strongly depends on the characteristics of the equilibrium model and of the driving wave. The absorption can produce efficient local heating of plasma under conditions as in the solar atmosphere.

Key words: Magnetohydrodynamics (MHD) – methods: numerical – Sun: corona – Sun: oscillations

1. Introduction

The solar atmosphere contains a wide variety of magnetic structures which can support MHD waves. Waves that are generated either by turbulent motions in the photosphere and chromosphere, or by global solar oscillations or by local releases of energy in reconnection events interact with these magnetic structures.

Propagating waves transport energy away from the region where they are generated into the ambient plasma, while dissipation causes a deposition of part of the wave energy in the plasma. The classic viscous or resistive damping of for example Alfvén waves in a uniform plasma is known to be a very inefficient way to transform wave energy irreversibly into heat in weakly dissipative plasmas with large values of the viscous and magnetic Reynolds numbers as in the solar plasma.

However, a more efficient mechanism for dissipating wave energy can occur in nonuniform magnetic plasmas, where resonant slow and resonant Alfvén waves can exist. In ideal MHD these resonant waves are confined to an individual magnetic surface without any interaction with neighbouring magnetic surfaces. Since each magnetic surface has its own local slow frequency and its own local Alfvén frequency, a nonuniform magnetic plasma can have two continuous ranges of frequencies corresponding to resonant slow waves and resonant Alfvén waves.

Dissipative effects cause coupling of the resonant magnetic surface to neighbouring magnetic surfaces. For large values of the viscous and the magnetic Reynolds numbers as in the solar atmosphere this coupling is weak and the local resonant slow oscillations and the local resonant Alfvén oscillations are characterized by steep gradients accross the magnetic surfaces. Excitation of these local slow oscillations or local Alfvén oscillations provides a means for dissipating wave energy which is far more efficient in weakly dissipative plasmas than classical resistive or viscous MHD wave damping in a uniform plasma. This mechanism of resonant wave damping was first put forward as a possible mechanism for heating the solar corona by Ionson (1978).

The excitation of the local resonant oscillations can be direct by driving motions in the magnetic surfaces or indirect by driving motions normal to the magnetic surfaces. The indirect excitation relies on global motions that transfer energy across the magnetic surfaces up to the resonant magnetic surface where the frequency of the global motion equals the local Alfvén frequency or local slow frequency. The excitation of the localised

Send offprint requests to: Á. Csík

⋆ On leave from Institute of Physics, P.O. Box 57, YU-11000 Beograd, Yugoslavia.

⋆⋆ On leave from Department of Astronomy, Eötvös University Budapest, Ludovika tér 2 H-1083 Budapest, Hungary.

⋆⋆⋆ Armagh Observatory, College Hill, Armagh, BT61 9DG, Northern Ireland.

resonant waves is indirect since we need magnetosonic waves that propagate across the magnetic surfaces to excite them.

Most studies on heating by indirect excitation have considered incoming fast magnetosonic waves that couple to local resonant Alfvén waves in a nonuniform plasma (Poedts, Goossens and Kerner (1989), Poedts, Goossens and Kerner (1990), Okretič and Čadež (1991)). Fast magnetosonic waves propagate almost isotropically as long as their high frequencies are above the cutoff frequency for fast waves. Slow magnetosonic waves are not considered an important means for transferring energy into the corona and for heating the plasma there, primarily because of the limited range of frequencies of the slow continuum waves. However, they can play a role when slow and fast magnetosonic waves that are generated in the photosphere interact with chromospheric magnetic structures and when slow and fast magnetosonic waves that are generated locally in the corona interact with coronal magnetic fields.

In this paper the focus is on the absorption of slow and fast incoming magnetosonic waves by coupling to local resonant slow magnetosonic waves in a nonuniform plasma. This process is studied for an equilibrium configuration which makes the mathematical analysis as simple as possible but still contains the basic physical ingredients.

The equilibrium model is specified in Sect. 2. In Sect. 3 we present the set of ideal MHD equations that govern the linear motions in a planar 1D equilibrium model. In this Sect. we also discuss the singularities in the differential equations of linear ideal MHD and their role for resonant wave damping. The solutions of the differential equation of linear ideal MHD in the two uniform plasma layers are also given. In Sect. 4 we explain how the analysis of resonant waves in dissipative layers (Sakurai, Goossens and Hollweg (1991), Goossens and Hollweg (1993), Goossens, Ruderman and Hollweg (1995) in what follows SGH, GH and GRH respectively) can be applied to obtain the solutions in the vicinity of the mathematical singularity of the ideal MHD equations. The definition of the absorption coefficient and the method for its computation are given in Sect. 5. In Sect. 6 we present our results and conclusions.

2. The equilibrium configuration

We consider a static 1D planar equilibrium model composed of two semi-infinite uniform plasma layers which embrace a nonuniform plasma layer. We use a system of Cartesian coordinates with the z-axis directed downward. The horizontal planes $z = 0$ and $z = L$ bound the nonuniform plasma layer from above and from below respectively. The plasma is uniform in the regions $z < 0$ (region 1) and $z > L$ (region 2). In the nonuniform plasma layer ($0 \leq z \leq L$) the equilibrium quantities depend on z only.

The magnetic field is assumed to be constant in the whole space and is oriented along the $x-$axis: $\mathbf{B_0} = (B_0, 0, 0)$. Gravity is neglected in the present analysis.

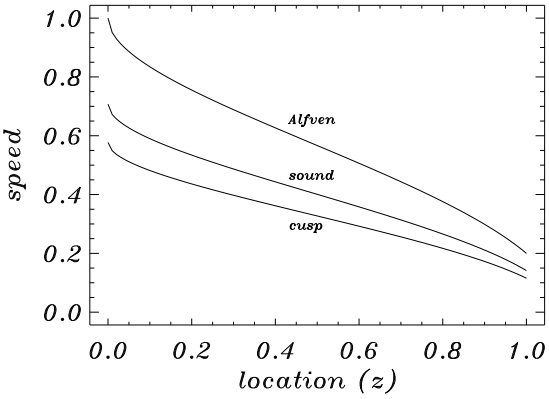

Fig. 1. The characteristic velocity profiles for the considered equilibrium state with $\beta = 0.6$ and $n = 0.5$

Since the magnetic pressure $p_m \equiv B_0^2/2\mu_0$ is constant, the thermal pressure p_0 is also constant and so is the plasma parameter $\beta = p_0/p_m$:

$$p_0 = \frac{1}{\gamma}\rho_0(z)v_s^2(z) = const. \tag{1}$$

In addition we can freely specify either the temperature T_0 or the density ρ_0.

Of course, $B_0 = const.$ implies that

$$\rho_0(z)v_A^2(z) = const. \quad \text{and} \quad \rho_0(z)v_c^2(z) = const.$$

The object of the present paper is to study the absorption of slow and fast magnetosonic waves by coupling to local resonant slow magnetosonic waves. The resonant slow waves are controlled by the local cusp frequency which is determined by the wave vector and the local cusp speed. Hence in the present context it is convenient to prescribe the variation of the square of the local cusp velocity v_c^2

$$v_c^2 = \frac{v_A^2 v_s^2}{v_A^2 + v_s^2} \tag{2}$$

as a function that is monotonous inside the nonuniform layer $0 \leq z \leq L$ and is constant elsewhere:

$$v_c^2(z) = \begin{cases} v_2^2 = const., & z \geq L \\ v_1^2 - \left(v_1^2 - v_2^2\right)\left(\frac{z}{L}\right)^n, & 0 \leq z \leq L \\ v_1^2 = const. & z \leq 0 \end{cases} \tag{3}$$

The expressions for density, local Alfvén speed and local sound speed take the simple forms:

$$\begin{aligned} \rho_0 &= \frac{\rho_{00} v_1^2}{v_c^2(z)}, \\ v_A^2 &= \left(1 + \tfrac{2}{\gamma\beta}\right) v_c^2(z) \\ v_s^2 &= \left(1 + \tfrac{\gamma\beta}{2}\right) v_c^2(z), \end{aligned} \tag{4}$$

where $v_c^2(z)$ is prescribed by Eqs (3). The dimensionless Alfvén, sound, and cusp speed as functions of coordinate z are shown in Fig. 1.

We use this model for studying the resonant absorption of magnetosonic waves in different structures in the solar atmosphere. The incoming wave is launched from the lower uniform layer $z > L$ with a prescribed frequency ω and a prescribed wave vector $\boldsymbol{k}$, and propagates towards the nonuniform layer. At the boundary $z = L$ the wave is partly reflected and partly transmitted. The energy of the transmitted wave is partly absorbed in the nonuniform plasma due to the resonant excitation of local waves. With our choice of the direction of the z-axis, the incident wave propagates in the negative z-direction and the reflected wave propagates in the positive z-direction. We do not want to consider leaky waves and restrict our analysis to waves that are evanescent in the upper uniform layer.

3. Governing equations and solutions

The driven waves are studied with the standard set of linearized equation of ideal MHD:

$$\begin{aligned}
&\frac{\partial \rho_1}{\partial t} + \nabla \cdot (\rho_0 \boldsymbol{v}_1) = 0,\\
&\rho_0 \frac{\partial \boldsymbol{v}_1}{\partial t} = -\nabla p_1 + \frac{1}{\mu_0}(\nabla \times \boldsymbol{B}_1) \times \boldsymbol{B}_0\\
&\qquad + \frac{1}{\mu_0}(\nabla \times \boldsymbol{B}_0) \times \boldsymbol{B}_1, \qquad (5)\\
&\frac{\partial \boldsymbol{B}_1}{\partial t} = \nabla \times (\boldsymbol{v}_1 \times \boldsymbol{B}_0)\\
&\frac{\partial p_1}{\partial t} + \boldsymbol{v}_1 \cdot \nabla p_0 = v_s^2 (\frac{\partial \rho_1}{\partial t} + \boldsymbol{v}_1 \cdot \nabla \rho_0)
\end{aligned}$$

An index '0' denotes an equilibrium quantity, while an index '1' denotes an Eulerian perturbation. Since the equilibrium quantities depend on z only we can Fourier analyze the perturbed quantities with respect to the ignorable spatial coordinates x and y and put them proportional to $exp(i(k_x x + k_y y))$ with k_x, and k_y the components of the horizontal wave vector. The present paper is concerned with the steady state of driven waves excited by an incoming wave with prescribed frequency ω so that the time dependency of all perturbed quantities is given by $exp(-i\omega t)$. Hence the perturbed quantities are written as:

$$f_1(x, y, z, t) = f(z) \mathrm{e}^{i(k_x x + k_y y - \omega t)}.$$

The Eqs. (5) can be reduced to two coupled ordinary differential equations for the normal component of the Lagrangian displacement $\xi_z \equiv i\, v_z/\omega$ and for the Eulerian perturbation of the total pressure $P \equiv p_1 + B_0 B_{1x}/\mu_0$:

$$D\frac{d\xi_z}{dz} = -C_1 P, \qquad \frac{dP}{dz} = C_2 \xi_z. \qquad (6)$$

The coefficient functions D, C_1, and C_2 are given by

$$\begin{aligned}
D &= \rho_0 (v_s^2 + v_A^2)(\omega^2 - \omega_c^2)(\omega^2 - \omega_A^2),\\
C_1 &= (\omega^2 - \omega_A^2)(\omega^2 - \omega_s^2) - \omega^2 v_A^2 k_y^2, \qquad (7)\\
C_2 &= \rho_0 (\omega^2 - \omega_A^2).
\end{aligned}$$

The Alfvén frequency ω_A, sound frequency ω_s, and cusp frequency ω_c are defined as

$$\omega_A = v_A k_x, \qquad \omega_s = v_s \sqrt{k_x^2 + k_y^2}, \qquad \omega_c = v_c k_x.$$

The set of ordinary differential equations has two mobile regular singularities at the positions where $D = 0$, this is at the positions where

$$\omega = \omega_c(z_c) \quad \text{or} \quad \omega = \omega_A(z_A). \qquad (8)$$

Since $\omega_c(z)$ and $\omega_A(z)$ are functions of z, the relations (8) define two continuous ranges of frequencies referred to as the slow continuum and the Alfvén continuum.

3.1. Solutions in the uniform layers

The solutions to the ordinary differential equations (6) can be obtained in closed analytic form for a uniform equilibrium state. For a uniform plasma the coefficient functions D, C_1 and C_2 are constants and it is straightforward to rewrite the set of ordinary differential equations of first order as a single ordinary differential equation of second order for P:

$$\frac{d^2 P}{dz^2} + \frac{C_1 C_2}{D} P = 0. \qquad (9)$$

Depending on the sign of $C_1 C_2/D$ the solutions are spatially propagating waves ($C_1 C_2/D > 0$) or spatially evanescent or exponentially growing waves ($C_1 C_2/D < 0$).

The object is to study how magnetosonic waves that are generated in the underlying uniform plasma propagate upward toward the nonuniform plasma layer and are partially absorbed there. This means that we have to choose k_x, k_y, and ω so that $C_1 C_2/D$ is positive. In that case we define the square of the $z-$component of the wave vector $\boldsymbol{k}$ as

$$k_z^2 \equiv \frac{C_1 C_2}{D} = \frac{(\omega^2 - \omega_I^2)(\omega^2 - \omega_{II}^2)}{(v_A^2 + v_s^2)(\omega^2 - \omega_c^2)}. \qquad (10)$$

The frequencies ω_I and ω_{II} are the cut-off frequencies for fast and slow magnetosonic waves in a uniform plasma. Their squares are given by

$$\omega_{I,II}^2 = \frac{1}{2}(v_A^2 + v_s^2)(k_x^2 + k_y^2) \left\{ 1 \pm \left[1 - \frac{4\omega_c^2}{(v_A^2 + v_s^2)(k_x^2 + k_y^2)} \right]^{\frac{1}{2}} \right\}.$$

In the lower uniform plasma layer the solution of Eq. (9) represents a superposition of two waves propagating in opposite directions along the $z-$axis

$$P = P^{(+)}\mathrm{e}^{ik_z(z-L)} + P^{(-)}\mathrm{e}^{-ik_z(z-L)}$$
$$\xi_z = \frac{ik_z}{C_2}P^{(+)}\mathrm{e}^{ik_z(z-L)} - \frac{ik_z}{C_2}P^{(-)}\mathrm{e}^{-ik_z(z-L)} \tag{11}$$

where all coefficients are constant and evaluated at $z = L$.

We do not want to consider leaky waves that transport energy toward infinite and restrict our analysis to waves that are evanescent in the upper uniform layer. This means that we have to choose k_x, k_y and ω so that C_1C_2/D is negative there and can be written as

$$C_1C_2/D = -\kappa^2$$

where κ is real and positive. The solutions that vanish in the limit $z \to -\infty$ are:

$$P = \mathrm{e}^{\kappa z}, \qquad \xi_z = \frac{\kappa}{C_2}\mathrm{e}^{\kappa z} \tag{12}$$

with all the coefficients evaluated at $z = 0$. The integration constants are choosen as to provide a unit total pressure perturbation at $z = 0$.

Let us return to the expression for $\omega_{I,II}$. It is well-known that $\omega_c^2 \le \omega_I^2 \le \omega_A^2 \le \omega_{II}^2$ for a uniform plasma. As a consequence we have two frequency windows for propagating magnetosonic waves in a uniform plasma, namely

$$\omega_c^2 \le \omega^2 \le \omega_I^2 \tag{13}$$

and

$$\omega^2 \ge \omega_{II}^2. \tag{14}$$

The first window corresponds to propagating slow magnetosonic waves, the second to propagating fast magnetosonic waves. Fast magnetosonic waves are practically isotropic under solar conditions $v_A \gg v_s$. Slow magnetosonic waves, however, are largely anisotropic. A clear manifestation of this anisotropy of slow magnetosonic waves is that the phase velocity and the group velocity have z-components of different sign so that an upward directed phase velocity corresponds to a downward directed group velocity.

The product of the $z-$components of the group velocity $V_{gz} \equiv \partial\omega/\partial k_z$ and the phase velocity $V_{pz} \equiv \omega/k_z$ can be written as

$$V_{gz}V_{pz} = \frac{(v_A^2 + v_s^2)(\omega^2 - \omega_c^2)^2}{(2\omega^2 - \omega_I^2 - \omega_{II}^2)(\omega^2 - \omega_c^2) - (\omega^2 - \omega_I^2)(\omega^2 - \omega_{II}^2)}. \tag{15}$$

A simple analysis shows that

$$V_{gz}V_{pz} > 0 \qquad \text{for fast waves,}$$
$$V_{gz}V_{pz} < 0 \qquad \text{for slow waves.} \tag{16}$$

Since the group velocity of a wave is related to the corresponding energy flux, expressions (16) show the sense of the energy transport with respect to the wave front motion, taken along the $z-$axis: the orientations are the same for fast waves and opposite for slow waves.

In an attempt to make the geometry of the wave propagation more visible, we introduce two propagation angles θ and ϕ related to the wave vector and the magnetic field as:

$$k_x = k\sin(\theta)\cos(\phi), \quad k_y = k\sin(\theta)\sin(\phi),$$
$$k_z = k\cos(\theta), \qquad \text{where} \qquad k^2 = k_x^2 + k_y^2 + k_z^2 \tag{17}$$

Here θ is the angle between the wave vector $\boldsymbol{k}$ and the direction of the nonuniformity and ϕ is the angle between the magnetic field and the horizontal wave vector.

Substituting expressions (17) into (10), we can solve Eq. (10) for the absolute value of the wave vector $\boldsymbol{k}$ as

$$k = \omega\left[\frac{1}{2}(v_A^2 + v_s^2) \pm \frac{1}{2}\left(v_A^4 + v_s^4 - 2v_A^2v_s^2\cos(2\alpha)\right)^{\frac{1}{2}}\right]^{-\frac{1}{2}} \tag{18}$$

where $\alpha = \cos^{-1}(\sin(\theta)\cos(\phi))$ is the angle between the magnetic field and the wave vector. In Eq. (18) the plus sign stands for the fast and the minus sign stands for the slow magnetosonic waves respectively.

In our computations we first fix the values of the driving frequency ω and of the propagation angles θ and ϕ. We then compute the absolute value of the wave vector from Eq. (18) depending on the type of the incoming wave (slow or fast). Using the value of k and angles θ and ϕ we can compute the components of the wave vector. Therefore we study the behaviour of an incoming wave with a prescribed wave frequency and with prescribed propagation angles θ and ϕ.

3.2. Solution in the nonuniform layer

The solutions of the ordinary differential equations that govern the linear motions cannot be obtained in closed analytic form in a nonuniform plasma. Numerical integration is required there. In addition, the prime purpose of this paper is to study the resonant damping of incoming magnetosonic waves by coupling to local resonant waves. In order for this phenomenon to occur the frequency of the incoming wave has to be within either the Alfvén or the slow continuum. Hence for the situation that is of interest to us the ideal MHD equations are singular. In ideal MHD the solutions for resonant waves are singular indicating that they can not be used for the description of resonant waves.

The inclusion of non-ideal effects removes the singularity from the equations but at the same time raise the order of the system of ordinary differential equations. A correct description of resonant wave behaviour requires the use of dissipative MHD. SGH (1991) and GRH (1995) show that numerical integration of the dissipative MHD equations can be avoided for weakly dissipative plasmas with very large values of the magnetic and viscous Reynolds numbers. For resonant MHD waves

the dissipative terms are only important in a narrow layer around the ideal resonant position. Outside this narrow layer the MHD waves are accurately described by the equations of ideal MHD. The analysis by SGH (1991) and GRH (1995)leads to a simple numerical scheme for the accurate computation of resonant MHD waves as was shown by Stenuit et al (1995).

For a fixed wave frequency ω and wave vector $\boldsymbol{k}$ the location of the possible resonances (cusp resonance alone or Alfvén and cusp resonance together) and the width of the dissipative layers are determined before hand. The solutions in the nonuniform plasma outside of the dissipative layers are obtained by numerical integration of Eqs. (6) starting from initial values for P and ξ_z at $z = 0$. These values are given by the analytical solutions (12) evaluated at the boundary of the region 1 as both, P and ξ_z, should be continuous at $z = 0$. The numerical integration of the two ordinary differential equations of first order of ideal MHD does not require any special treatment and can be done by a simple Runge Kutta Merson scheme. In the vicinity of a resonant point the jump conditions (see SGHR method from Sect. 4) are applied to connect the solutions accross the dissipative layer. Integration of Eqs. (6) is continued up to the boundary of region 2 at $z = L$.

Once the solutions are obtained at $z = L$, say P_L and ξ_{zL} we can relate them to the analytical solutions (11) by requiring their continuity at $z = L$ which yields the following expressions for the amplitudes $P^{(+)}$ and $P^{(-)}$:

$$P^{(+)} = \frac{k_z P_L - iC_2\xi_L}{2k_z} \qquad P^{(-)} = \frac{k_z P_L + iC_2\xi_L}{2k_z} \tag{19}$$

which are related to the waves with $V_{pz} > 0$ and $V_{pz} < 0$ respectively.

4. Solutions close to singularities

As it was already mentioned in Sect. 1 and in Sect. 3, Eqs. (6) are valid only away from the resonant surfaces defined by Eqs. (8). Close to the ideal singularity we use the SGHR method to determine the solutions. This means that we use the ideal MHD equations everywhere except within a comparatively narrow dissipative layer around the resonances where the ideal solutions for P and ξ_z tend to diverge and the dissipative terms should be included in the equations.

In this paper, we are not particularly interested in the details of the solutions within the dissipative layer and all we need to know is how to cross the layer containing the singularity during the numerical computations of ξ_z and P. For this purpose, we use connection formulae (GRH 1995) that relate the solutions for both, P and ξ_z, at the end points of the dissipative layer. A brief description of how this is done for the cusp and the Alfvén resonant dissipative layers is given below. The dominant dissipation is taken to arise from the isotropic electric resistivity η.

4.1. The cusp resonance

When dissipation is included, an analysis by SGH (1991) and GRH (1995) leads to the following set of simplified differential equations for resonant driven slow waves in dissipative MHD around the cusp resonant point z_c

$$\begin{aligned}
&\left[s\Delta_c - i\omega\eta\frac{\omega_c^2}{\omega_A^2}\frac{d^2}{ds^2}\right]\frac{d\xi_z}{ds} = \frac{\omega_c^4}{\rho_0 v_A^2\omega_A^2}P,\\
&\left[s\Delta_c - i\omega\eta\frac{\omega_c^2}{\omega_A^2}\frac{d^2}{ds^2}\right]\frac{dP}{ds} = 0
\end{aligned} \tag{20}$$

where the new variable is $s = z - z_c$, η is the electric resistivity and $\Delta_c = d(\omega^2 - \omega_c^2)/ds$. In Eqs. (20) all coefficients have their values taken at $s = 0$.

The solutions of Eqs. (20) yield the jump conditions, which connect the solutions accross the dissipative resonant layer for both the Lagrangian displacement ξ_z and the total pressure perturbation P:

$$\begin{aligned}
&[\xi_z]_c = -i\pi\frac{\omega_c^4}{|\Delta_c|\rho_0 v_A^2\omega_A^2}P,\\
&[P]_c = 0
\end{aligned} \tag{21}$$

where all equilibrium quantities in (21) are taken at $z = z_c$. The second relation in (21) represents the conservation law for the Eulerian perturbation of the total pressure .

The extent of the dissipative layer can be measured by the parameter δ_c as in GRH (1995). The value of δ_c is obtained by equating the dissipative and the non-dissipative terms in the left hand side of Eqs. (20). The asymptotic analysis in GRH (1995) shows that dissipation is important only within the interval $[-5\delta_c, 5\delta_c]$ around the resonant point $z = z_c$. Outside this interval, the dissipative term becomes negligible in comparison to the ideal terms in (20) and the ideal MHD equations can be used. In particular, when isotropic electric resistivity η is considered as the dominant dissipative process, the width of the dissipative layer is proportional to:

$$\delta_c = \left(\frac{\omega\eta}{|\Delta_c|}\frac{\omega_c^2}{\omega_A^2}\right)^{1/3}. \tag{22}$$

4.2. The Alfvén resonance

An analogous procedure can be applied to the Alfvén resonance, which yields the approximate dissipative differential equations for ξ_z and P close to $z = z_A$

$$\begin{aligned}
&\left[s\Delta_A - i\omega\eta\frac{d^2}{ds^2}\right]\frac{d\xi_z}{ds} = \frac{k_y^2}{\rho_0}P,\\
&\left[s\Delta_A - i\omega\eta\frac{d^2}{ds^2}\right]\frac{dP}{ds} = 0
\end{aligned} \tag{23}$$

where $s = z - z_A$, $\Delta_A = d(\omega^2 - \omega_A^2)/ds$ and all equilibrium quantities have their values taken at $z = z_A$.

Eqs. (23) imply that the conservation law for resonant Alfvén waves is the same as for resonant slow waves. The jump conditions for the Alfvén resonance are:

$$\begin{aligned}
&[\xi_z]_A = -i\pi\frac{k_y^2}{|\Delta_A|\rho_0}P,\\
&[P]_A = 0.
\end{aligned} \tag{24}$$

Jump conditions (24) are applied to connect the solutions for P and ξ_z accross the interval $[-5\delta_A, 5\delta_A]$ around the Alfvén singularity. An expression δ_A is determined by

$$\delta_A = \left(\frac{\omega\eta}{|\Delta_A|}\right)^{1/3}. \tag{25}$$

5. Calculation of the absorption coefficient

To study the resonant absorption of magnetosonic waves, we derive an expression for the absorption coefficient $\mathscr{A}$ from the amplitudes of the incident and the reflected waves at $z = L$.

The absorption coefficient is defined as

$$\mathscr{A} \equiv 1 - \frac{|\mathscr{F}_z^{(r)}|}{|\mathscr{F}_z^{(i)}|} \tag{26}$$

where $\mathscr{F}_z^{(i)}$ and $\mathscr{F}_z^{(r)}$ are the $z-$components of the energy flux densities of the incident and the reflected wave respectively. $\mathscr{F}_z^{(i)}$ and $\mathscr{F}_z^{(r)}$ can be expressed in terms of the $z-$components of the group velocities $V_{gz}^{(i,r)}$ and the total wave energy densities $w^{(i,r)}$ as

$$\mathscr{F}_z^{(i,r)} = V_{gz}^{(i,r)} w^{(i,r)} \tag{27}$$

The terms 'incident wave' and 'reflected wave' are therefore determined by the sign of the $z-$component of the group velocity in the sense that incident waves have $V_{gz} \equiv V_{gz}^{(i)} < 0$ while reflected waves have $V_{gz} \equiv V_{gz}^{(r)} > 0$. $V_{gz}^{(i)}$ and $V_{gz}^{(r)}$ are equal in absolute value as they are related to the same location of the plasma. Consequently, they cancel out in the expressions (26) and (27) for calculating the absorption coefficient.

According to the inequalities (16) the sign of the z-component of the phase velocity and the z-component of the group velocity are the same for fast magnetosonic waves and opposite for slow magnetosonic waves. It means that fast magnetosonic waves carry energy in the direction of the wave propagation, and slow magnetosonic waves carry energy in the opposite direction of the wave propagation.

In Eqs. (11) the amplitudes $P^{(+)}$ and $P^{(-)}$ are related to the waves propagating in the positive z-direction and the negative z-direction respectively. This means that $P^{(+)}$ and $P^{(-)}$ are the amplitudes of the reflected and the incident wave respectively when the wave is a fast magnetosonic wave. In the case of slow magnetosonic waves the situation is reversed. The amplitudes $P^{(+)}$ and $P^{(-)}$ are now related to the incident and the reflected wave respectively.

Therefore, we can write the total pressure amplitudes $P^{(i)}$ and $P^{(r)}$ for the incident and the reflected wave as

$$\begin{array}{lll} P^{(i)} = P^{(-)}, \quad P^{(r)} = P^{(+)} & & \text{for fast waves} \\ P^{(i)} = P^{(+)}, \quad P^{(r)} = P^{(-)} & & \text{for slow waves} \end{array} \tag{28}$$

As we know the total pressure amplitudes of the incident and the reflected wave for both the slow and fast magnetosonic waves, we can calculate the related energy densities needed in (27) and the absorption coefficient (26).

The total wave energy density

$$w^{(i,r)} = w_k^{(i,r)} + w_t^{(i,r)} + w_m^{(i,r)} \tag{29}$$

is the sum of the kinetic $w_k^{(i,r)}$, thermal $w_t^{(i,r)}$ and magnetic energy $w_m^{(i,r)}$ given as

$$w_k = \frac{1}{2}\rho_0 < v^2(\boldsymbol{r},t) >, \quad w_t = \frac{v_s^2}{2\rho_0} < \rho^2(\boldsymbol{r},t) >,$$

$$w_m = \frac{1}{2}\rho_0 v_A^2 < b^2(\boldsymbol{r},t) > .$$

The averaged values of perturbation squares in the above expressions are equal to one half of the related amplitude squares in the case of harmonic waves. Thus:

$$\begin{aligned} w_k &= \tfrac{1}{4}\rho_0|v|^2, \ \text{ with } \ |v|^2 = |v_x|^2 + |v_y|^2 + |v_z|^2, \\ w_t &= \tfrac{v_s^2}{4\rho_0}|\rho|^2, \\ w_m &= \tfrac{1}{4}\rho_0 v_A^2|b|^2, \ \text{ with } \ |b|^2 = |b_x|^2 + |b_y|^2 + |b_z|^2. \end{aligned} \tag{30}$$

where $\boldsymbol{b} \equiv \boldsymbol{B}/B_0$ and the superscripts (r,i) indicate the reflected and the incident wave respectively, are omitted.

The perturbed quantities in (30) can all be expressed in terms of the Eulerian perturbation of total pressure for the region 2 with a uniform plasma as

$$\begin{aligned} v_x &= \frac{1}{\rho_0}\frac{k_x}{\omega}\left[1 - \frac{v_A^2(k_y^2+k_z^2)}{\omega^2-\omega_A^2}\right]P \equiv a_1(\omega,\boldsymbol{k})P \\ v_y &= \frac{1}{\rho_0}\frac{k_y\omega}{\omega^2-\omega_A^2}P \equiv a_2(\omega,\boldsymbol{k})P \\ v_z &= \frac{1}{\rho_0}\frac{k_z\omega}{\omega^2-\omega_A^2}P \equiv a_3(\omega,\boldsymbol{k})P \\ \rho &= \frac{1}{v_s^2}\left[1 - \frac{v_A^2(k_y^2+k_z^2)}{\omega^2-\omega_A^2}\right]P \equiv a_4(\omega,\boldsymbol{k})P \\ b_x &= \frac{1}{\rho_0}\frac{k_y^2+k_z^2}{\omega^2-\omega_A^2}P \equiv a_5(\omega,\boldsymbol{k})P \\ b_y &= -\frac{1}{\rho_0}\frac{k_xk_y}{\omega^2-\omega_A^2}P \equiv a_6(\omega,\boldsymbol{k})P \\ b_z &= -\frac{1}{\rho_0}\frac{k_xk_z}{\omega^2-\omega_A^2}P \equiv a_7(\omega,\boldsymbol{k})P \end{aligned} \tag{31}$$

When we substitute expressions (31) into (30), we can write

$$w_k = \frac{1}{4}\rho_0(a_1^2+a_2^2+a_3^2)|P|^2 \equiv \mathscr{W}_k|P|^2$$

$$w_t = \frac{v_s^2}{4\rho_0}a_4^2|P|^2 \equiv \mathscr{W}_t|P|^2$$

$$w_m = \frac{1}{4}\rho_0 v_A^2(a_5^2+a_6^2+a_7^2)|P|^2 \equiv \mathscr{W}_m|P|^2$$

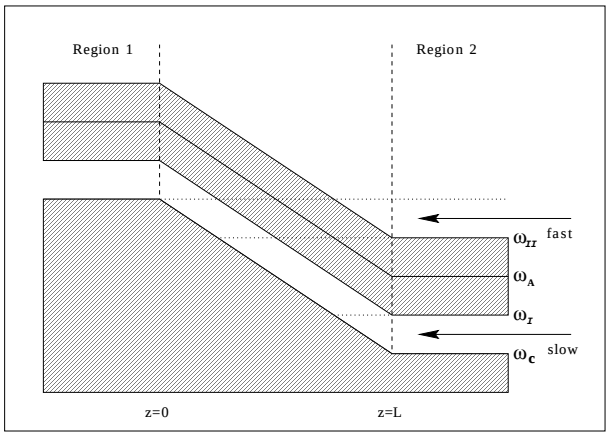

Fig. 2. A schematical view of the considered wave propagation domains for slow and fast magnetosonic waves.

so that the total energy densities (29) for the incident and the reflected wave become:

$$w^{(i,r)} = \left(\mathscr{W}_k + \mathscr{W}_t + \mathscr{W}_m\right) |P^{(i,r)}|^2 \tag{32}$$

Consequently, the absorption coefficient (26) can be reduced to the simple expression

$$\mathscr{A} = 1 - \frac{|P^{(r)}|^2}{|P^{(i)}|^2} \tag{33}$$

with $P^{(r)}$ and $P^{(i)}$ given by relations (28).

6. Results and conclusions

The results are obtained for the equilibrium model specified by (3). We have taken $\beta = 0.6$, $\gamma = 5/3$, $n = 0.5$ and $v_A(L)/v_A(0) = 0.2$ which corresponds to the density ratio $\rho(L)/\rho(0) = 25$. Lengths, velocities and time are expressed in terms of L, $v_A(0)$ and $\tau \equiv L/v_A(0)$, respectively.

The absorption coefficient $\mathscr{A}$ is calculated for a given wave frequency ω and a wave vector $\boldsymbol{k} = (k_x, k_y, k_z)$ that satisfy the equation (10) for propagating waves in the region 2 and the condition $\kappa^2 > 0$ for evanescent waves in the region 1. The wave vector components are further related to the wave propagation angles ϕ and θ according to expressions (17).

Since we do not intend to consider the Alfvén resonance alone, the frequencies and the wave vectors are chosen in such a way that they satisfy the condition $\omega \leq \omega_c(0) \equiv v_1 k_x$. This means that the driving frequency remains smaller than the maximal value of the cusp frequency as shown schematically in Fig. 2.

Thus we investigate how the properties of the wave absorption due to the resonant excitation of slow and Alfvén continua by slow and fast magnetosonic waves, depend on the wave frequency ω and the propagation angles θ and ϕ. The angle θ varies from 0° to 90° while the angle ϕ ranges between 0° and 180°. In our model, however, the wave characteristics are symmetric

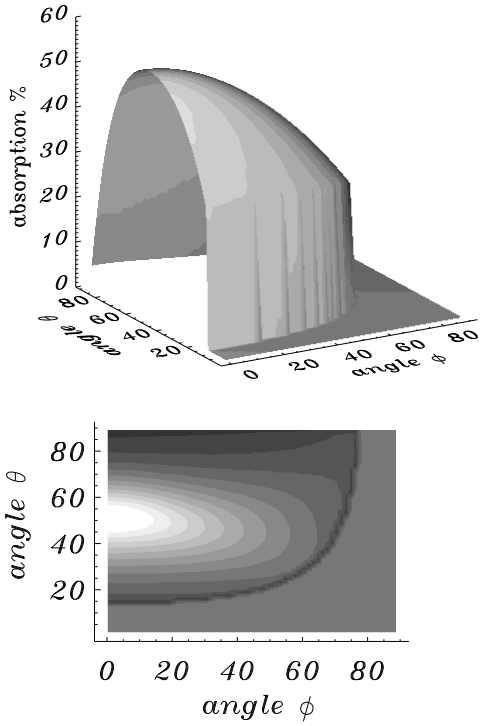

Fig. 3. a The dependence of the absorption coefficient on the incident angle θ and the azimuth angle ϕ for slow MHD waves. **b** The top view of the surface $\mathscr{A}(\theta, \phi)$ showing the boundary of the computational domain. The dimensionless wave frequency is $\omega = 0.8$.

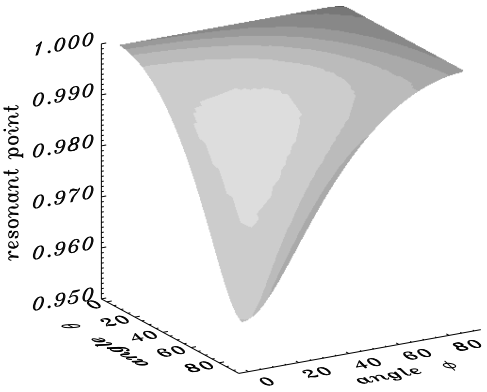

Fig. 4. The location of the cusp resonance depending on angles θ and ϕ for slow MHD waves with $\omega = 0.8$

with respect to $\phi = 90°$ since k_x and k_y appear only through their squares. For this reason, $90° \geq \phi \geq 0°$ is taken in calculations.

In the case of a magnetosonic driving wave with an initially prescribed frequency ω, the location where the considered type of resonance occurs will depend on the $x-$component of the wave vector i.e. on the propagation angles according to (17). However, for certain values of θ and ϕ the driving frequency can be very close to either the lower end points of the cusp ($\omega \rightarrow \omega_c(1)$) and the Alfvén continua ($\omega \rightarrow \omega_A(1)$) re-

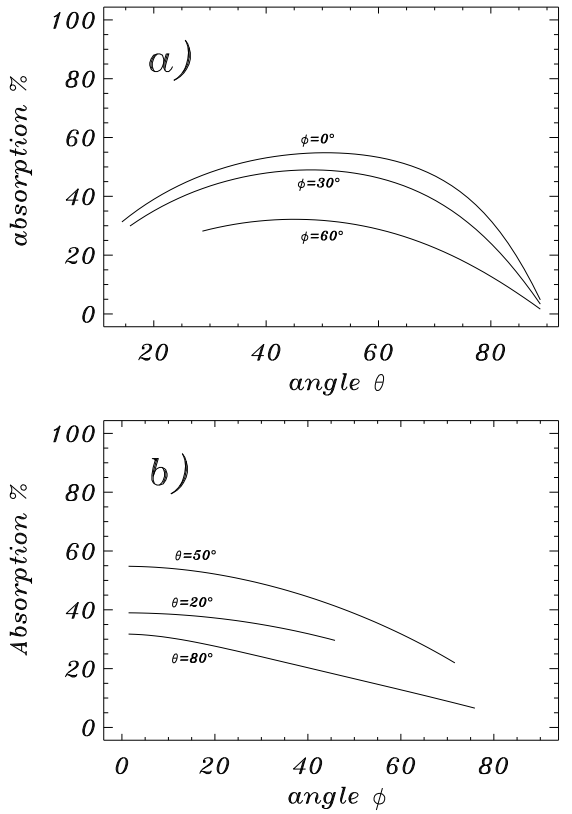

Fig. 5a and b. Absorption of slow MHD waves with the frequency $\omega = 0.8$. **a** The dependence of the absorption coefficient $\mathscr{A}$ on the incident angle θ at three indicated azimuthal angles ϕ. **b** The dependence of the absorption coefficient $\mathscr{A}$ on the azimuthal angle ϕ at three indicated incident angles θ.

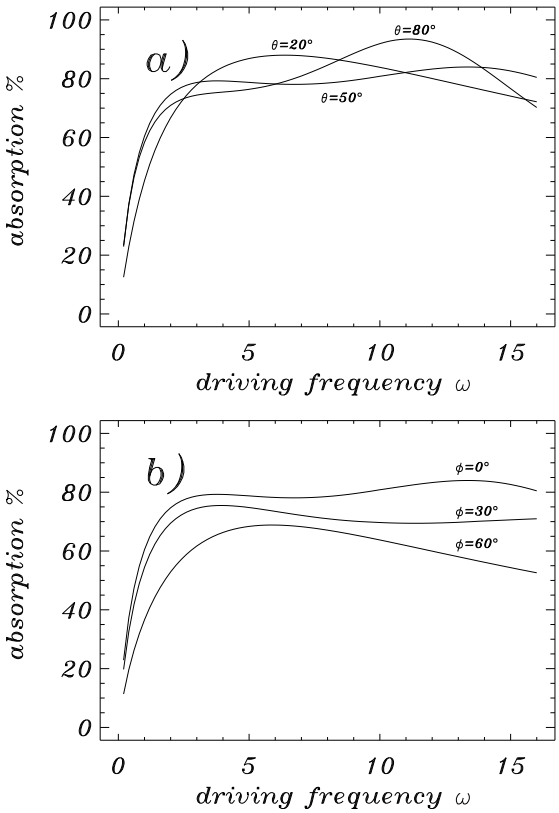

Fig. 6a and b. The dependence of the absorption coefficient $\mathscr{A}$ on the wave frequency ω for slow MHD waves for: **a** $\phi = 0°$ and **b** $\theta = 50°$ and other parameters as indicated.

spectively, or to the upper end point of the cusp continuum ($\omega \to \omega_c(0)$).

In the first case, the cusp, resp. the Alfvén resonance, occurs very close to the boundary $z = 1$ ($z_c \to 1$, $z_A \to 1$) meaning that the whole lower uniform layer is practically in resonance. This then results into computational difficulties. In the second case the cusp resonance occurs practically at $z = 0$ ($z_c \to 0$) i.e. at the limit when the region 1 becomes transparent for the considered waves, and computational difficulties arise again.

We first study how incoming slow magnetosonic waves are absorbed by coupling to local resonant slow waves. Results for the absorption rate are shown in Fig. 3a as a function of θ and ϕ for a typical dimensionless wave frequency $\omega = 0.8$.

In our model an incoming propagating slow magnetosonic wave enters into the nonuniform layer, and propagates up to the resonant point, where it is partially absorbed by the cusp resonance. After the resonance the wave becomes evanescent (see Fig. 2).

For values of angles θ and ϕ which produce the cusp resonance close to $z = 1$, the value of the absorption coefficient is artifically put to zero. In Fig. 4, a 3D plot shows the location of the cusp resonance $z_c(\theta, \phi)$ with $\omega = 0.8$ and for the parameter domain. The domain of angles θ and ϕ where $z_c \to 1$, clearly coincides with the domain in which the absorption coefficient can not be calculated. Therefore a cut appears in Fig. 3a which separates the regions where the absorption can be and can not be calculated. The profile of the cut is shown in Fig. 3b showing the vertical view at the surface from Fig. 3a.

The absorption rate reaches values close to 60% at $\phi = 0°$ and θ around 50°. For other values of θ and ϕ it smoothly decreases to well below 10% where the absorption surface is cut and ends abruptly.

The absorption coefficient is shown as a function of θ (for fixed ϕ) in Fig. 5a and as a function of ϕ (for fixed θ) in Fig. 5b. The curves end at angles where $z_c \to 1$ as noted above.

The dependency of the absorption of slow waves on the wave frequency is presented in Fig. 6: a) for $\phi = 0°$ and several values of θ and b) for $\theta = 50°$ and taking ϕ as a parameter. These two fixed values where chosen as they yield the maximal value for $\mathscr{A}$ in Fig. 3. The plots now show that the absorption increases with the frequency to high values close to 90%.

Next we investigate the absorption of incoming fast magnetosonic waves by coupling to localised resonant slow waves. Since these waves have frequencies that are above the upper cutoff frequency $\omega_{II}(1)$ at $z = 1$, they reach first the Alfvén resonance z_A and then the cusp resonance z_c that is located within the layer so that $1 \geq z_A > z_c$. Thus both resonances contribute to the absorption of fast waves provided the wave frequency ω

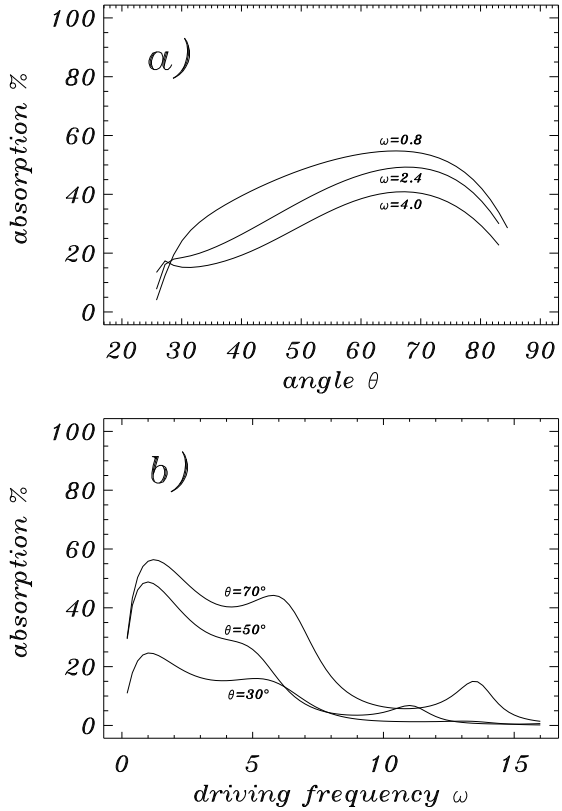

Fig. 7a and b. Absorption of fast MHD waves with $\phi = 0°$. **a** The dependence of the absorption coefficient $\mathscr{A}$ on the incident angle θ at three indicated wave frequencies ω. **b** The dependence of the absorption coefficient $\mathscr{A}$ on the wave frequency ω at three indicated angles of incidence θ.

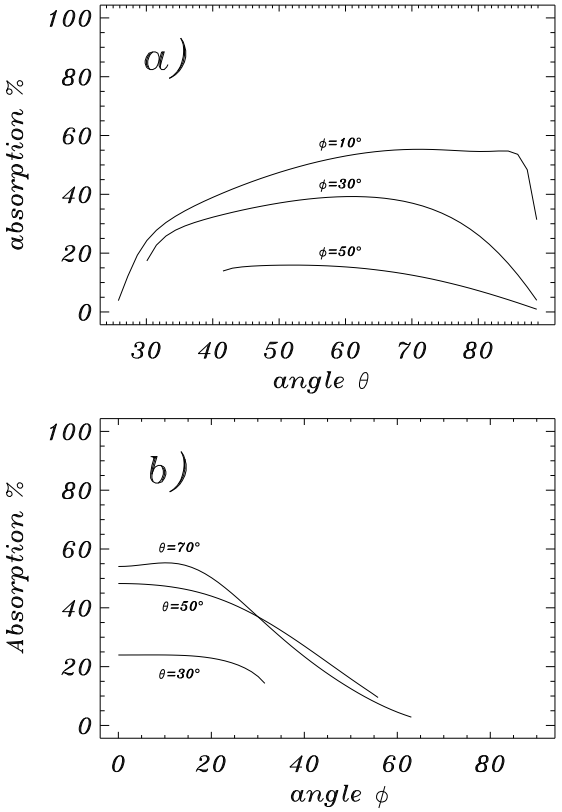

Fig. 9a and b. Absorption of fast MHD waves with the frequency $\omega = 0.8$. **a** The dependence of the absorption coefficient $\mathscr{A}$ on the incident angle θ at three indicated azimuthal angles ϕ. **b** The dependence of the absorption coefficient $\mathscr{A}$ on the azimuthal angle ϕ at three indicated incident angles θ.

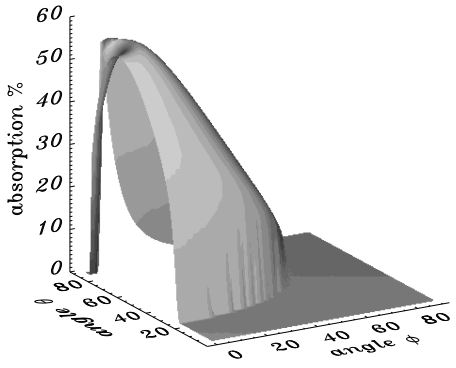

Fig. 8. The dependence of the absorption coefficient on the incident angle θ and the azimuth angle ϕ for fast MHD waves.

does not exceed the value of the cusp frequency at $z = 0$, i.e. for $\omega_c(0) \geq \omega \geq \omega_{II}(1)$. At higher frequencies when $\omega \geq \omega_c(0)$ the absorption occurs from the Alfvén resonance solely, because $\omega_c(0)$ is the maximal value of the cusp frequency.

The only way of avoiding the Alfvén resonance for fast waves is to consider waves propagating with $\phi = 0°$. Eqs. (17) show that for $\phi = 0°$ the $y-$component of the wave vector is zero. Hence, the Alfvén singularity disappears from Eqs (6). The absorption coefficient for three different frequencies is shown in Fig. 7a while Fig. 7b shows the absorption as a function of the frequency of the incoming wave for three different angles θ in the case of $\phi = 0°$. A general conclusion is that the absorption of fast waves with $k_y = 0$ is less efficient when compared to the absorption of slow waves and does not exceed 60%. The curves end again where $z_c \to 0$.

Finally, if $\phi \neq 0°$ the Alfvén resonance also occurs and the dependency of the absorption coefficient on θ and ϕ is shown in Fig. 8. In this case the wave dynamics is complex. An incoming propagating fast magnetosonic wave propagates up to the point, where its frequency equals to the cutoff frequency ω_{II} for fast waves. From there on the wave tunnels until it hits the Alfvén resonance, where it is partially absorbed. It further tunnels up to the point where the wave frequency equals to the cutoff frequency ω_I for slow waves. From this point on the wave propagates up to the cusp resonant point where it is partially absorbed. Subsequently the wave becomes evanescent (see Fig. 2).

For $\theta \to 90°$ and $\phi \to 0°$, the Alfvén resonance occurs very close to the lower boundary layer at $z = 1$, and computational difficulties arise, so we set the value of the absorption coefficien to zero. Outside of the domain of θ and ϕ where the absorption surface is present, the value of the absorption is set to zero again. The reason is that for those angles the driving frequency of the

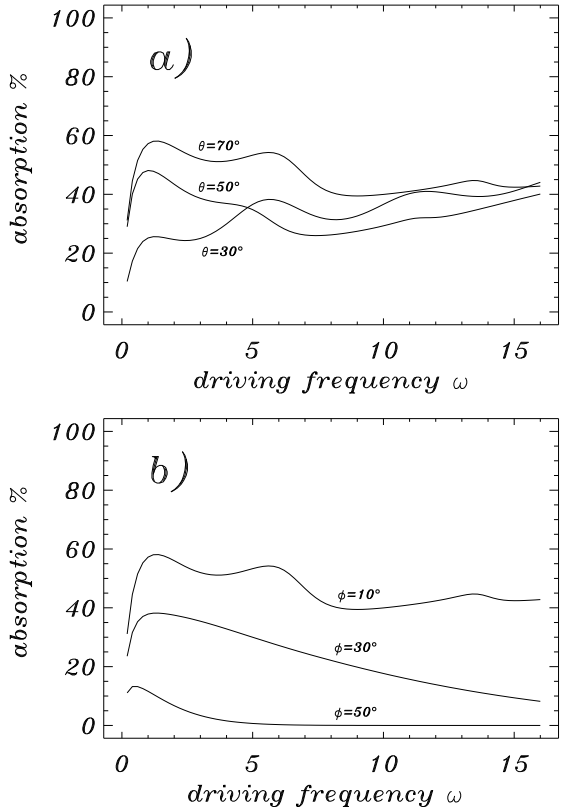

Fig. 10a and b. The dependence of the absorption coefficient $\mathscr{A}$ on the wave frequency ω for fast MHD waves for: **a** $\phi = 10^\circ$ and **b** $\theta = 70^\circ$ and other parameters as indicated.

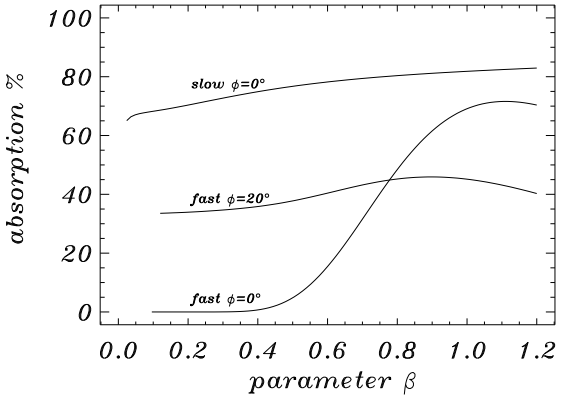

Fig. 11. The dependence of the absorption coefficient $\mathscr{A}$ on the parameter β for fast and for slow MHD waves when: $\omega = 6$ and $\theta = 50^\circ$ and ϕ as indicated.

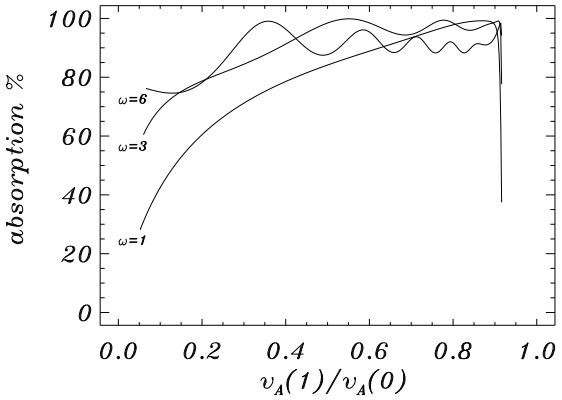

Fig. 12. The dependence of the absorption coefficient $\mathscr{A}$ on the ratio of the Alfvén speeds $v_A(1)/v_A(0)$ for slow MHD waves when: $\beta = 0.6$, $\theta = 50^\circ$ and $\phi = 0^\circ$.

fast wave is higher than the maximal value of the cusp frequency $\omega_c(0)$, or it is close to $\omega_c(0)$ which causes the cusp resonance to be very close to $z = 0$, therefore we exclude these possibilities.

The cross sectional plots in Fig. 9 clearly indicate that the absorption is again most efficient at incident angles θ in the interval $50^\circ - 60^\circ$ and that it decreases with ϕ. Fig. 10 shows that waves are more efficiently absorbed at lower frequencies.

The results obtained so far are for an equilibrium with $\beta = 0.6$ and for $v_A(1)/v_A(0) = 0.2$. They show that the highest values of the absorption coefficient occur for $\theta \approx 50^\circ$ and for $\omega \approx 6$. The variation of the absorption coefficient as a function of β is shown in Fig. 11.

The dependence of the absorption coefficient on the ratio $v_A(1)/v_A(0)$ is given in Fig. 12 for three wave frequencies for slow magnetosonic wave only. The values of the remaining parameters are $\phi = 0^\circ$, $\theta = 50^\circ$ and $\beta = 0.6$.

Up to now, we have studied general properties of absorption of magnetosonic waves by coupling to local resonant slow waves in a nonuniform plasma layer that separates two uniform regions. To put the present results in the solar context, we can take region 1 as the corona, region 2 as the photosphere, where the incoming magnetosonic waves are generated and the nonuniform layer as the chromosphere.

Let us take $v_s(0) = 100\,\mathrm{km/s}$ and $v_s(1) = 8\,\mathrm{km/s}$ for the sound speeds corresponding to temperatures $T_0(0) \approx 10^6\,K$ and $T_0(1) \approx 6,000\,K$ for the corona and the photosphere respectively and $\beta = 0.6$. We then obtain for the related Alfvén speeds $v_A(0) \approx 140\,\mathrm{km/s}$ and $v_A(1) \approx 10\,\mathrm{km/s}$ or $v_A(1)/v_A(0) \approx 0.1$ for their ratio. Fig. 12 shows that a wave with a dimensionless frequency $\omega \approx 1$ can be absorbed close to 50% if the the directional angles are $\theta = 50^\circ$ and $\phi = 0^\circ$ at the Alfvén speed ratio of ≈ 0.1. The value of $\omega \approx 1$ then corresponds to a period t_0:

$$t_o = \frac{2\pi}{\omega}\frac{L}{v_A(0)} \approx \frac{L}{23}[s]$$

if the thickness of the layer L is given in kilometers. Thus, if $L = 2,300\,\mathrm{km}$ which is a typical value for the thickness of the chromosphere, we obtain $t_o \approx 2\,min$ for the wave period which does not differ significantly from the period of the observed solar p-oscillations. In other words, the solar p-oscillations can play a role in the process of chromospheric heating through the mechanism of enhanced absorption of MHD waves at the cusp resonance.

Another example of significant absorption of magnetosonic waves by coupling to local resonant waves occurs when the incoming waves are generated locally in the solar corona. To examine this possibility, we consider both uniform layers to be located in the corona and separated by a nonuniform layer with a thickness of L. Let the waves propagate through the region with a lower temperature of $T_0(1) \approx 10^6\,K$ and be evanescent in the other domain with the higher temperature of $T_0(0) \approx 2 \times 10^6\,K$. Taking β = 0.6, the related values for the sound and the Alfvén speeds are then: $v_s(1)$ = 100 km/s, $v_s(0)$ = 140 km/s, $v_A(1) \approx$ 140 km/s and $v_A(0) \approx$ 200 km/s respectively. The period t_0 of the waves that are absorbed in the layer, is then $t_0 \approx 0.03\,L/\omega\,[s]$, where ω is the dimensionless frequency and L is given in kilometers. We can now take $L \approx 60,000$ km and ω = 6 which gives a period of t_0 = 5 min for the wave. Its absorption follows from Fig. 12 to be about 90% at $v_A(1)/v_A(0) \approx 0.7$.

To conclude, the resonant absorption of magnetosonic waves coupled to local resonant magnetosonoc waves under the considered conditions can be an efficient mechanism for the coronal heating, mostly by slow magnetosonic waves. Fast magnetosonic waves are less absorbed at this resonance.

Acknowledgements. V.Čadež acknowledges the financial support by the 'Onderzoeksfonds K.U.Leuven' (senior research fellowship F/95/62). Á. Csík is grateful to the Hungarian Soros Foundation and the 'Onderzoeksfonds K.U.Leuven'. This work was partly carried out while R. Erdélyi was a doctoral student financed by the Research Council of the Katholieke Universiteit Leuven, Belgium (OT/92/8). The support by the K.U.L. Research Council is greatly acknowledged. R. Erdélyi was also supported by the grant GR/K43315 from the PPARC of the U.K.

References

Goossens,M. and Hollweg,J.V. 1993, Solar Physics. 145, 19.
Goossens, M., Ruderman, M. S. and Hollweg, J.V. 1995, Solar Physics, 157, 75.
Ionson,J.A. 1978, ApJ. 226, 650.
Okretič, V. and Čadež, V.M. 1991, Physica Scripta, 43, 306.
Poedts, S., Goossens, M. and Kerner, W. 1989, Solar Physics, 123, 83.
Poedts, S., Goossens, M. and Kerner, W. 1990, Astrophysical Journal, 360, 279.
Sakurai, T., Goossens, M. and Hollweg, J.V. 1991, Solar Physics, 133, 247.
Stenuit, H., Erdélyi, R. and Goossens, M. 1995, Solar Physics, 161, 139.

This article was processed by the author using Springer-Verlag LaTeX A&A style file *L-AA* version 3.